LETTERS

Phase-locking and environmental fluctuations generate synchrony in a predator–prey community

David A. Vasseur[1] & Jeremy W. Fox[2]

Spatially synchronized fluctuations in system state are common in physical and biological systems ranging from individual atoms[1] to species as diverse as viruses, insects and mammals[2–10]. Although the causal factors are well known for many synchronized phenomena, several processes concurrently have an impact on spatial synchrony of species, making their separate effects and interactions difficult to quantify. Here we develop a general stochastic model of predator–prey spatial dynamics to predict the outcome of a laboratory microcosm experiment testing for interactions among all known synchronizing factors: (1) dispersal of individuals between populations; (2) spatially synchronous fluctuations in exogenous environmental factors (the Moran effect); and (3) interactions with other species (for example, predators) that are themselves spatially synchronized. The Moran effect synchronized populations of the ciliate protist *Tetrahymena pyriformis*; however, dispersal only synchronized prey populations in the presence of the predator *Euplotes patella*. Both model and data indicate that synchrony depends on cyclic dynamics generated by the predator. Dispersal, but not the Moran effect, 'phase-locks' cycles, which otherwise become 'decoherent' and drift out of phase. In the absence of cycles, phase-locking is not possible and the synchronizing effect of dispersal is negligible. Interspecific interactions determine population synchrony, not by providing an additional source of synchronized fluctuations, but by altering population dynamics and thereby enhancing the action of dispersal. Our results are robust to wide variation in model parameters representative of many natural predator–prey or host–pathogen systems. This explains why cyclic systems provide many of the most dramatic examples of spatial synchrony in nature.

Understanding what causes populations to fluctuate in synchrony is important because synchrony can increase extinction risk in metapopulations[11,12], facilitate recolonization waves in cyclic populations[13], and increase or decrease the stability of food webs[14,15]. Although the synchronizing effects of dispersal and the Moran effect have been well studied[16–20], relatively little effort has focused on the operation of these mechanisms in the presence of species interactions (but see refs 13, 20–23). Besides providing an additional source of synchronized fluctuations, interspecific interactions can introduce high-amplitude cycles in population dynamics through nonlinear feedbacks and time delays[24]. Many of the most dramatic examples of spatial synchrony in nature come from species or systems that cycle through time, including measles and pertussis outbreaks, larch bud moth outbreaks, Fennoscandian voles and Canadian lynx–hare cycles[2,3,7–10], suggesting that interspecific interactions generating cycles may be a crucial ingredient to understanding spatial synchrony.

We predicted the separate and interactive effects of different processes on spatial synchrony by developing a stochastic spatial predator–prey model based on the standard Rosenzweig–MacArthur model (Methods). Our model incorporated key features of predator–prey biology (density-dependent prey growth and time-limited predator activity budget) known to drive the dynamics of many natural predator–prey systems[25]. We simulated a factorial experiment crossing the presence/absence of dispersal, the Moran effect and the predator to examine their effects on prey synchrony. We conducted 10,000 Monte Carlo simulations of this experiment by varying five key model parameters randomly so as to thoroughly sample a large region of the ecologically relevant parameter space (see Supplementary Information).

The model predicts that the Moran effect synchronizes prey dynamics, but dispersal significantly increases prey synchrony only with predators present (Fig. 1a, b and Supplementary Information). The dispersal–predator interaction arises because predators generate oscillations that are easily synchronized by dispersal. The dispersal–predator interaction is a statistical signature of what is commonly described in dynamical systems theory as 'phase-locking', whereby coupling of periodic or chaotic oscillators entrains their phases and periods[1–4,26,27]. In the absence of dispersal, initially synchronous cycles desynchronize ('decohere') when predator and prey simultaneously reach low densities; subtle differences in noise at the nadir of the cycle can lead to large differences in the timing of subsequent peaks and consequently loss of synchrony (Fig. 2b and Supplementary Information). In the presence of dispersal, cycles tend to emerge from the nadir in lock-step because any differences in density are eliminated by a net flow of individuals from the higher-density to the

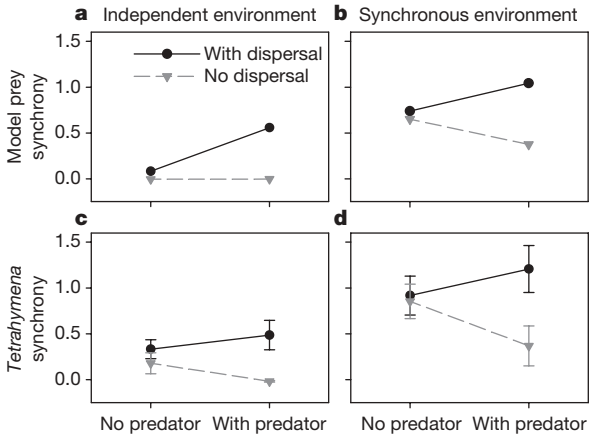

Figure 1 | Three-way interaction plot of the impact of dispersal, the Moran effect and predators on *Tetrahymena* synchrony. a–d, Results from our theoretical model (**a**, **b**) and our experimental microcosms (**c**, **d**) are shown. Points represent the mean *z*-transformed Pearson cross-correlation (±1 s.e.m.). In the experiment, both dispersal and the Moran effect significantly increase synchrony, but dispersal does so only in the presence of predators.

[1]Department of Ecology and Evolutionary Biology, Yale University, New Haven, Connecticut 06520, USA. [2]Department of Biological Sciences, University of Calgary, Calgary, Alberta T2N 1N4, Canada.

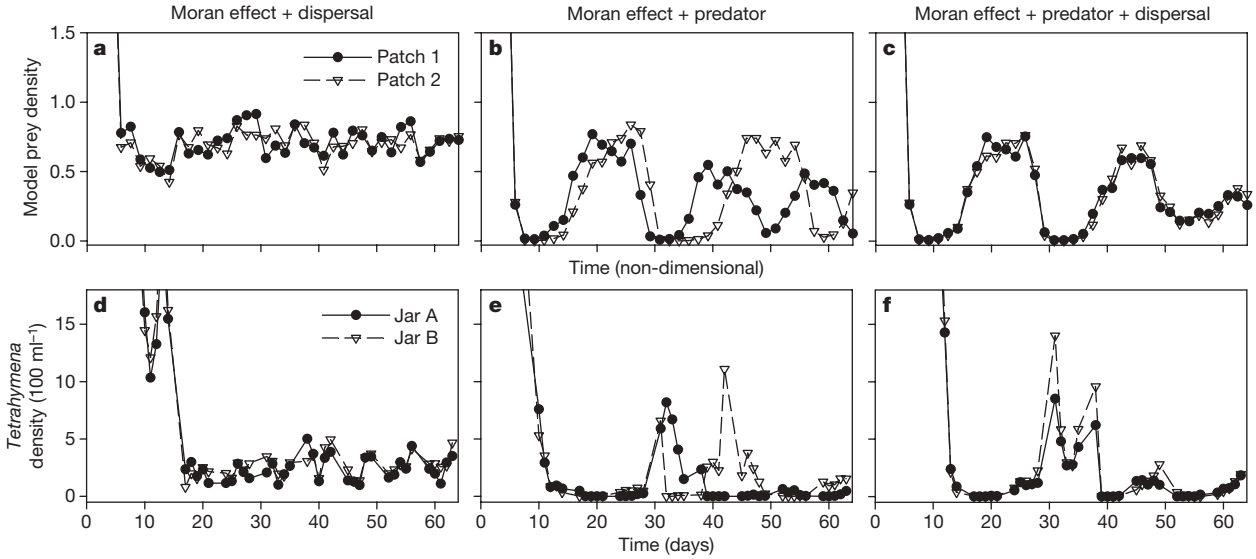

Figure 2 | Temporal dynamics of *Tetrahymena*. **a**–**f**, Results from pairs of jars experiencing the Moran effect and dispersal (**a**, **d**), predators (**b**, **e**), or predators and dispersal (**c**, **f**) are shown. Panels **a**–**c** give illustrative dynamics from our theoretical model, and **d**–**f** give illustrative dynamics from our experimental microcosms. Adding predators to the theoretical model and experimental *Tetrahymena* cultures generates cyclic dynamics. In the presence of dispersal, cyclic dynamics are entrained by phase-locking. Across panels **a**–**c** the same initial conditions and stochastic perturbations were used to highlight the effect of predators and dispersal.

lower-density patch (Fig. 2c and Supplementary Information); the greater the density difference between patches the stronger the flow. In contrast, when predators are absent, prey densities exhibit stochastic fluctuations around carrying capacity (Fig. 2a) that allow little scope for dispersal to generate synchrony because density differences are random, non-cyclic, and are continually created. Dispersal of only prey or predators produces results similar to those observed when both species disperse, emphasizing that the dispersal–predator interaction arises from phase-locking of predator–prey cycles, not from prey tracking predators that are themselves synchronized through predator dispersal (Supplementary Information).

In contrast to dispersal, the Moran effect does not generate phase-locking[2,4,26,27] and is slightly weakened by predator–prey cycles (Fig. 1a, b and Supplementary Information). The Moran effect operates by synchronously perturbing systems away from their intrinsically generated trajectories. In the presence of any source of spatially independent stochasticity, even perfectly synchronous environmental perturbations are unlikely to ensure that cycles emerge from the nadir in lock-step (Supplementary Information). Furthermore, the synchronizing effect of these perturbations does not increase with the density difference between the patches.

To test the model predictions we conducted a laboratory microcosm experiment. We grew the ciliate protist *Tetrahymena pyriformis* in paired batch cultures (habitat patches) using a system that closely matches model assumptions (Supplementary Information). We manipulated dispersal (no dispersal, or periodic exchanges of a small volume of culture medium between paired cultures), the Moran effect (spatially synchronous or spatially independent temperature fluctuations) and species interactions (absence or presence of the predatory ciliate *Euplotes patella*) in a full factorial design, as in the model simulations. This is the first factorial experiment manipulating all possible sources of spatial population synchrony.

The model proved capable of quantitatively predicting the experimental results (Fig. 1). As predicted, both dispersal and the Moran effect significantly increased the synchrony of *Tetrahymena* ($F_{1,36} = 6.5$, $P = 0.02$; $F_{1,36} = 20.3$, $P < 0.001$, respectively). Crucially, a significant interaction between dispersal and predators ($F_{1,36} = 4.8$, $P = 0.04$) indicated that dispersal was a much stronger synchronizing force in the presence of predators; dispersal had no significant effect on prey synchrony in the absence of predators ($F_{1,22} = 0.4$, $P = 0.5$). This interaction arose because predators decreased *Tetrahymena* synchrony in the absence of dispersal and increased it in the presence of dispersal, as predicted by the model. The remaining main effect and interaction terms were all nonsignificant, although we observed the predicted trend for predators to weaken the Moran effect (Fig. 1).

We found a strong qualitative match between the model predictions and experimentally observed treatment effect sizes across a large range of ecologically relevant parameter space (Fig. 3). Eighty-six per cent of Monte Carlo replicates predicted the three significant treatment effects found in our experiment (dispersal, the Moran effect, and the dispersal–predator interaction) to be the three strongest effects in the analysis of variance (ANOVA).

Our data rule out alternative mechanisms by which predators might enhance the synchronizing effect of dispersal. First, dispersal might synchronize predator dynamics, leading to increased prey synchrony because prey are impacted by fluctuations in predator density.

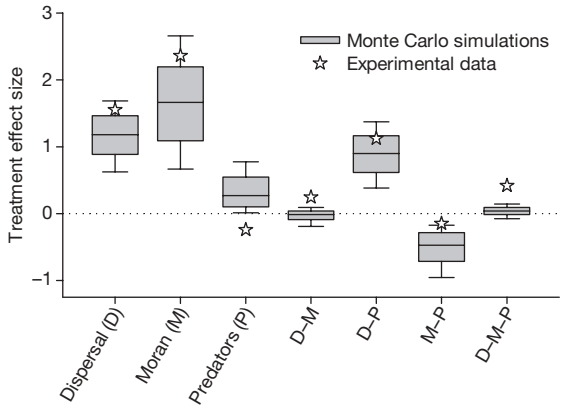

Figure 3 | The distribution of treatment effects generated by Monte Carlo simulation of 10,000 random parameterizations of the Rosenzweig–MacArthur model. Boxes represent the median, 25/75th, and 10/90th percentiles of the effect-size distribution and stars represent the experimental data. Treatment effects were calculated as the cumulative difference between, for example, dispersal against non-dispersal treatments (see Supplementary Information). Five model parameters were drawn from uniform intervals: attack rate (2.33, 5), dispersal rate (0.05, 0.25), process error standard deviation σ_ξ (0.05, 0.25), environment error standard deviation σ_ε (0.3, 0.9), and the correlation of the predator's and the prey's environment (−1, 1).

However, only the Moran effect significantly increased synchrony of the predator *Euplotes* (Fig. 4; $F_{1,16} = 13.6$, $P = 0.002$), suggesting that dispersal does not synchronize *Tetrahymena* indirectly by synchronizing the predator. Second, predators did not increase the strength of the Moran effect on prey synchrony, as would be expected if increased predator synchrony indirectly increased prey synchrony. Finally, lack of a significant correlation between prey and predator synchrony ($\rho = 0.05$, $t_{18} = 0.013$, $P = 0.99$) directly demonstrates that predator synchrony did not drive the synchrony of *Tetrahymena*.

In our experiment, *Euplotes* increased the temporal variability of *Tetrahymena* densities (coefficient of variation; $F_{1,84} = 49.6$, $P < 0.0001$). It is possible that increased temporal variability could increase spatial variability and thereby strengthen the synchronizing effect of dispersal, because the net prey dispersal rate is proportional to the difference in prey density between patches. However, our model demonstrates that simply increasing the variability of prey densities does not alter the impact of dispersal (Supplementary Information).

Instead, predators increased the synchronizing effect of dispersal by generating large-amplitude predator–prey cycles (Fig. 2d–f and Supplementary Fig. 7). The observed cycles were characterized by long periods with both predator and prey at low densities making them particularly susceptible to decoherence (Fig. 2e, f and Supplementary Information). However, in the presence of dispersal, cycles tended to emerge from the nadir nearly in lock-step, as predicted by the model (Fig. 2f). On average, paired prey populations emerged from the first cycle nadir (first non-zero prey sample density following first run of ≥2 consecutive samples with zero density) 1 day apart in the presence of dispersal and 2.5 days apart in the absence of dispersal, a significant difference (generalized linear model for Poisson-distributed data, $F_{1,18} = 5.68$, $P = 0.02$). In contrast, when predators were absent prey densities exhibited stochastic fluctuations around carrying capacity (Fig. 2d).

To test directly the ability of dispersal to synchronize emergence from the cycle nadir, we conducted a second, independent experiment (Supplementary Information). This experiment initiated replicate paired cultures slightly out of phase near the nadir of the predator–prey cycle, with half the replicates experiencing dispersal. As predicted by the model, in the absence of dispersal the difference in prey density between paired cultures increased as the 'leading' prey population emerged first from the cycle nadir and exhibited accelerating growth to high density. The prey density difference subsequently decreased as the leading prey population approached peak density and decelerated, allowing the 'trailing' prey population to (temporarily) catch up. Dispersal slowed prey growth in the leading patch and accelerated prey growth in the trailing patch, causing synchronous emergence from the cycle nadir and preventing the prey density difference from reaching large values. The results of this second experiment demonstrate that the model captures the detailed dynamical mechanisms linking dispersal to cycle synchrony in the first experiment.

Our results provide the first experimental demonstration of phase-locking of predator–prey cycles and extend the range of oscillatory dynamical systems in which phase-locking is known. Our results support previous work suggesting that dispersal is a more effective synchronizing agent in the presence of cyclic dynamics[4,13,21,27].

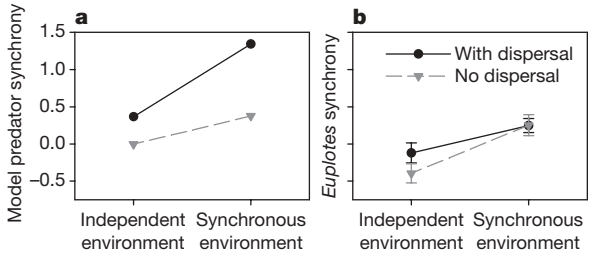

Figure 4 | Two-way interaction plot of the impact of dispersal and the Moran effect on predator synchrony. a, b, Results from our theoretical model (**a**) and our experimental microcosms (**b**) are shown. Points represent the mean *z*-transformed Pearson correlation (±1 s.e.m.). In the experiment, only the Moran effect significantly increases synchrony of the predator *Euplotes*.

Although the Moran effect significantly increased synchrony of both *Tetrahymena* and *Euplotes*, we found no evidence of environmental tracking in either species, or in our model simulations (Supplementary Fig. 8). Synchronous environmental forcing synchronizes population fluctuations by producing synchronous perturbations away from the intrinsically generated population trajectory. The Moran effect therefore can synchronize populations without population densities tracking environmental fluctuations[28]. Ciliates only noticeably track temperature fluctuations when maximum temperatures are sufficiently high to cause mass mortality[29].

In our experiment we found no significant effect of dispersal on *Euplotes* synchrony, in contrast to the model predictions (Fig. 4). This discrepancy may be due to lack of statistical power, as four replicates were lost as a result of predator extinction and *Euplotes* densities often were at or below the detection threshold for our sampling protocol.

Much previous work considers how coupling synchronizes oscillations[1]. Our work highlights the converse: oscillations enable coupling to produce synchrony. Our results provide a simple, general explanation for why many of the most dramatic examples of spatial synchrony in ecology comprise synchronized predator–prey oscillations. Like most examples of spatial synchrony, including Huygens' clocks, firing of the sinoatrial node in the mammalian heart, flashing of fireflies and light emission in lasers[1], it is the underlying oscillations that provide the scope for synchrony. Anthropogenic disturbances that alter or eliminate population cycles, such as vaccination against pathogens, climate change and species extirpations, may alter spatial synchrony and have unexpected consequences for species persistence.

METHODS SUMMARY

We conducted a fully crossed factorial experiment on the effect of dispersal, the Moran effect and predators on the synchrony of *T. pyriformis* dynamics in paired culture jars. Dispersal was accomplished by manual transfer of 10% of the experimental medium three times per week. We randomly varied the incubation temperature of culture jars on a daily basis between 20 and 30 °C according to prescribed schedules. Paired jars receiving the Moran effect experienced identical variability, whereas the remainder experienced independent variability. The predator treatment consisted of the addition of 15 individuals of *E. patella* to each jar in a pair on day 3 of the experiment. Each of the eight treatment combinations were replicated six times for a total of forty-eight experimental units. *Tetrahymena* and *Euplotes* densities were sampled each weekday using published methods[30], until day 64 of the experiment. We calculated the Pearson correlation of the first-order differences of *Tetrahymena* and *Euplotes* densities and conducted ANOVAs on the Fisher's *z*-transformed correlations.

We simulated a Rosenzweig–MacArthur predator–prey model in two patches and using the same eight treatment combinations as in the experiment. The experimental system matches key model assumptions (Supplementary Information). The equations were modified to include natural mortality in the prey, diffusive dispersal of individuals across patches, spatially correlated stochastic environmental fluctuations affecting background mortality rates, and process noise (a phenomenological description of other, spatially independent sources of random variation, including demographic stochasticity). We simulated the model for 2,048 time steps using a Runge–Kutta 4th/5th order algorithm, holding the stochastic parameters constant within each time step. We calculated synchrony of prey and predators in the manner described for the experiment, using only the latter 1,024 time-steps to ensure that initial transients had subsided. We conducted 10,000 Monte Carlo simulations in random multivariate parameter space to determine the robustness of our results (Supplementary Information).

Full Methods and any associated references are available in the online version of the paper at www.nature.com/nature.

Received 20 May; accepted 10 June 2009.
Published online 22 July 2009.

1. Strogatz, S. H. *SYNC: How Order Emerges From Chaos in the Universe, Nature and Daily Life* (Hyperion, 2003).
2. Ranta, E., Kaitala, V., Lindström, J. & Linden, H. Synchrony in population dynamics. *Proc. R. Soc. Lond. B* **262**, 113–118 (1995).

3. Liebhold, A., Koenig, W. D. & Bjørnstad, O. N. Spatial synchrony in population dynamics. *Annu. Rev. Ecol. Evol. Syst* **35,** 467–490 (2004).
4. Bjørnstad, O. N., Ims, R. A. & Lambin, X. Spatial population dynamics: analyzing patterns and processes of population synchrony. *Trends Ecol. Evol.* **14,** 427–432 (1999).
5. Moran, P. A. P. The statistical analysis of the Canadian lynx cycle. *Aust. J. Zool.* **1,** 291–298 (1953).
6. Grenfell, B. T. *et al.* Noise and determinism in synchronized sheep dynamics. *Nature* **394,** 674–677 (1998).
7. Rohani, P., Earn, D. J. D. & Grenfell, B. T. Opposite patterns of synchrony in sympatric disease metapopulations. *Science* **286,** 968–971 (1999).
8. Ims, R. A. & Andreassen, H. P. Spatial synchronization of vole population dynamics by predatory birds. *Nature* **408,** 194–196 (2000).
9. Bjørnstad, O. N. Cycles and synchrony: two historical 'experiments' and one experience. *J. Anim. Ecol.* **69,** 869–873 (2000).
10. Peltonen, M., Liebhold, A. M., Bjørnstad, O. N. & Williams, D. W. Spatial synchrony in forest insect outbreaks: roles of regional stochasticity and dispersal. *Ecology* **83,** 3120–3129 (2002).
11. Heino, M., Kaitala, V., Ranta, E. & Lindström, J. Synchronous dynamics and rates of extinction in spatially structured populations. *Proc. R. Soc. Lond. B* **264,** 481–486 (1997).
12. Earn, D. J. D., Rohani, P. & Grenfell, B. T. Persistence, chaos and synchrony in ecology and epidemiology. *Proc. R. Soc. Lond. B* **265,** 7–10 (1998).
13. Blasius, B., Huppert, A. & Stone, L. Complex dynamics and phase synchronization in spatially extended ecological systems. *Nature* **399,** 354–359 (1999).
14. Rooney, N., McCann, K., Gellner, G. & Moore, J. C. Structural asymmetry and the stability of diverse food webs. *Nature* **442,** 265–269 (2006).
15. Vasseur, D. A. & Fox, J. W. Environmental fluctuations can stabilize food web dynamics by increasing synchrony. *Ecol. Lett.* **10,** 1066–1074 (2007).
16. Hudson, P. J. & Cattadori, I. M. The Moran effect: a cause of population synchrony. *Trends Ecol. Evol.* **14,** 1–2 (1999).
17. Ripa, J. Analysing the Moran effect and dispersal: their significance and interaction in synchronous population dynamics. *Oikos* **89,** 175–187 (2000).
18. Engen, S. & Sæther, B.-E. Generalizations of the Moran effect explaining spatial synchrony in population fluctuations. *Am. Nat.* **166,** 603–612 (2005).
19. Vasseur, D. A. Environmental colour intensifies the Moran effect when population dynamics are spatially heterogeneous. *Oikos* **116,** 1726–1736 (2007).
20. Ripa, J. & Ranta, E. Biological filtering of correlated environments: towards a generalised Moran theorem. *Oikos* **116,** 783–792 (2007).
21. Cazelles, B. & Boudjema, G. The Moran effect and phase synchronization in complex spatial community dynamics. *Am. Nat.* **157,** 670–676 (2001).
22. Cattadori, I. M., Haydon, D. T. & Hudson, P. J. Parasites and climate synchronize red grouse populations. *Nature* **433,** 737–741 (2005).
23. Abbott, K. C. Does the pattern of population synchrony through space reveal if the Moran effect is acting? *Oikos* **116,** 903–912 (2007).
24. Kendall, B. E. *et al.* Why do populations cycle? A synthesis of statistical and mechanistic modeling approaches. *Ecology* **80,** 1789–1805 (1999).
25. Hassell, M. P., Lawton, J. H. & Beddington, J. R. Components of arthropod predation. I. The prey death-rate. *J. Anim. Ecol.* **45,** 135–164 (1976).
26. Jansen, V. A. A. Phase locking: another cause of synchronicity in predator–prey systems. *Trends Ecol. Evol.* **14,** 278–279 (1999).
27. Jansen, V. A. A. The dynamics of two diffusively coupled predator–prey populations. *Theor. Popul. Biol.* **59,** 119–131 (2001).
28. Ranta, E., Lundberg, P., Kaitala, V. & Laakso, J. Visibility of the environmental noise modulating population dynamics. *Proc. R. Soc. Lond. B* **267,** 1851–1856 (2000).
29. Petchey, O. L. Environmental colour affects aspects of single-species population dynamics. *Proc. R. Soc. Lond. B* **267,** 747–754 (2000).
30. Fox, J. W. Testing a simple rule for dominance in resource competition. *Am. Nat.* **159,** 305–319 (2002).

Supplementary Information is linked to the online version of the paper at www.nature.com/nature.

Acknowledgements A. Gonzalez, E. McCauley and P. Morin provided comments on an earlier version of the manuscript. J. Scharein, T. Janes and J. MacNeil provided laboratory assistance. Funding was provided by Alberta Ingenuity and NSERC postdoctoral fellowships to D.A.V. and by an NSERC Discovery Grant and an Alberta Ingenuity New Faculty Award to J.W.F.

Author Contributions Both authors conceived the experiment and analysed the results. D.A.V. conceived and analysed the model. Both authors wrote the paper.

Author Information Reprints and permissions information is available at www.nature.com/reprints. Correspondence and requests for materials should be addressed to D.A.V. (david.vasseur@yale.edu).

METHODS

Experimental methods. Experimental units comprised pairs of 80 ml culture jars containing a solution of sterilized local spring water, 0.2 g l^{-1} of Protozoan Pellets (standardized pellets of crushed, dried plant matter produced by Carolina Biological Supply), and one wheat seed. Protozoan Pellets and wheat seeds provide energy and nutrients for bacteria, which are consumed by *Tetrahymena*. The eight treatment combinations were replicated six times, yielding $n = 48$ experimental units. Twenty-four hours before inoculation with *Tetrahymena*, three species of bacteria were added to each jar: *Bacillus subtilis*, *Enterobacter aerogenes* and *Bacillus cereus*; other unidentified bacteria were added with the protists. On day 0, *T. pyriformis* stock culture (1 ml) was added to each jar (stock culture density 5,858.7 ml^{-1}). On day 3 of the experiment, 15 individuals per jar of *E. patella* were added to the 'predator' treatments by micropipette. Beginning on day 3, densities of *Tetrahymena* and *Euplotes* in small samples (~0.2 ml) were determined daily on weekdays using published methods[30]. The culture medium was refreshed weekly, beginning on day 4, by replacing 9 ml experimental medium with 10 ml fresh sterile medium; the difference accounted for loss due to sampling. The experiment continued until day 64, resulting in 44 observations per jar. Dispersal was accomplished by exchanging 8 ml medium between jars within a pair every Monday, Wednesday and Friday after sampling. This dispersal regime imposes density-independent (diffusive) dispersal characterized by equal per-capita dispersal rates for predators and prey.

Environmental fluctuations were accomplished daily by moving jars between 20 and 30 °C incubators according to prescribed schedules. Each schedule comprised 38 days at 20 °C and 26 days at 30 °C permuted by a random series possessing a reddened spectrum ($1/f^{0.5}$) (see ref. 19). This introduced a natural level of temporal autocorrelation into environmental fluctuations and ensured a consistent mean temperature for each jar (24.1 °C). We discarded and replaced two schedules prescribing incubation at 30 °C for more than 8 days in a 10 day period to better enable persistence of *Euplotes*. Jar pairs experiencing synchronized temperature fluctuations followed the same schedule; otherwise, jars followed independent schedules. Different replicate pairs within both synchronized and independent treatments experienced different time series of temperature fluctuations to avoid confounding environmental synchrony with the unique properties of any particular temperature time series.

We calculated the synchrony of *Tetrahymena* and *Euplotes* densities (x) within experimental units as the Pearson product-moment correlation (ρ) of the first-order differences, $r(t) = x(t+1) - x(t)$. We measured synchrony using cross-correlations rather than phase differences because our time series were too short to allow precise estimation of cycle phase. We measured synchrony in the same fashion in our theoretical model, so the experimental data directly test model predictions.

We conducted a three-factor ANOVA on the Fisher's z-transformed correlations, $z = 0.5\ln[(1+\rho)/(1-\rho)]$, to test for differences in synchrony across treatments. Inspection of the $r(t)$ series revealed a highly synchronized initial (transient) decline in *Tetrahymena* across all jars. We removed the first 12 days of data from the analysis to ensure that this synchronous transient did not dominate our results. Removing more than 12 days of initial data did not qualitatively alter our results and produced only very minor quantitative changes. In four replicate pairs containing both *Tetrahymena* and *Euplotes*, densities dropped below our detection threshold in at least one jar and did not recover; these replicates were excluded from all analyses. Inspection of residuals for all statistical analyses indicated conformity with distributional assumptions.

Theoretical model. The modified Rosenzweig–MacArthur model of prey N and predators P in patch i is given by the non-dimensional model:

$$\frac{dN_i}{dt} = N_i(1-N_i) - m_{N_i}N_i - \frac{aN_iP_i}{N_i+N_0} + d(N_j - N_i) + \varepsilon_{N_i}N_i$$

$$\frac{dP_i}{dt} = \frac{eaN_iP_i}{N_i+N_0} - m_{P_i}P_i + d(P_j - P_i) + \varepsilon_{P_i}P_i$$

where $i = 1, 2$ and $i \neq j$. Values for the attack rate $a = 3.0$, assimilation efficiency $e = 0.5$, and half-saturation density $N_0 = 0.3$ were chosen to generate predator–prey cycles that qualitatively mimic those seen in the experiment (Figs 1–3). Their exact values have little impact on the results, provided that they generate a limit cycle or damped oscillations in the absence of stochasticity (Supplementary Information).

Dispersal was controlled by the diffusive rate d and was equal to 0.15 (or 0) for both predators and prey. We imposed synchronized or independent fluctuations in the background per-capita mortality rates (m) according to $m_{N_i}(t) = 0.25\exp[\xi_i(t)]$ and $m_{P_i}(t) = 0.5\exp[\xi_i(t)]$ where ξ_i are discrete, normally distributed random variables with $\mu_\xi = 0$ and $\sigma_\xi = 0.6$ (see ref. 15 for rationale). In treatments without predators, P_i were initialized at zero, otherwise P_i and N_i were chosen randomly on the intervals (0.1, 0.2) and (0.5, 1.0), respectively.

Independent process error was imposed on each population by a discrete random normal variable ε with $\mu_\varepsilon = 0$ and $\sigma_\varepsilon = 0.15$. Our description of process error generates temporal variance in population size proportional to the square of mean population size, independent of spatially correlated environmental fluctuations and predator–prey cycles. This variance-mean scaling relationship is broadly consistent with theoretical arguments and empirical data[31].

31. Vasseur, D. A. & Gaedke, U. Spectral analysis unmasks synchronous and compensatory dynamics in phytoplankton communities. *Ecology* **88**, 2058–2071 (2007).